Article

Biomineral-Inspired Colloidal Liquid Crystals: From Assembly of Hybrids Comprising Inorganic Nanocrystals and Organic Polymer Components to Their Functionalization

Published as part of the Accounts of Chemical Research special issue "Self-Assembled Nanomaterials".

Masanari Nakayama* and Takashi Kato*

Read Online

ACCESS | Metrics & More | Article Recommendations

CONSPECTUS: Bioinspired organic/inorganic synthetic composites have been studied as high-performance and functional materials. In nature, biominerals such as pearls, teeth, and bones are self-organized organic/inorganic composites. The inorganic components are composed of calcium carbonate ($CaCO_3$) and hydroxyapatite (HAp), while the organic components consist of peptides and polysaccharides. These composites are used as structural materials in hard biological tissues. Biominerals do not show significantly higher performances than synthetic composites such as glass-fiber- or carbon-fiber-reinforced plastics. However, biominerals consist of environmentally friendly and biocompatible components that are prepared under mild conditions. Moreover, they form elaborate nanostructures and self-organized hierarchical structures. Much can be learned about material design from these biomineral-based hierarchical and nanostructured composites to assist in the preparation of functional materials.

Inspired by these biological hard tissues, we developed nanostructured thin films and bulk hybrid crystals through the self-organization of organic polymers and inorganic crystals of $CaCO_3$ or HAp. In biomineralization, the combination of insoluble components and soluble acidic macromolecules controls the crystallization process. We have shown that poly(acrylic acid) (PAA) or acidic peptides called polymer additives induce the formation of thin film crystals of $CaCO_3$ or HAp by cooperation with insoluble organic templates such as chitin and synthetic polymers bearing the OH group. Moreover, we recently developed $CaCO_3$- and HAp-based nanostructured particles with rod and disk shapes. These were obtained in aqueous media using a macromolecular acidic additive, PAA, without using insoluble polymer templates. At appropriate concentrations, the anisotropic particles self-assembled and formed colloidal liquid-crystalline (LC) phases.

LC materials are generally composed of organic molecules. They show ordered and mobile states. The addition of stimuli-responsive properties to organic rod-like LC molecules led to the successful development of informational displays, which are now widely used. On the other hand, colloidal liquid crystals are colloidal self-assembled dispersions of anisotropic organic and inorganic nano- and micro-objects. For example, polysaccharide whiskers, clay nanosheets, gibbsite plate-shaped particles, and silica rod-shaped particles exhibit colloidal LC states.

In this Account, we focused on the material design and hierarchical aspects of biomineral-based colloidal LC polymer/inorganic composites. We describe the design and preparation, nanostructures, and self-assembled behavior of these new bioinspired and biocompatible self-organized materials. The characterization results for these self-assembled nanostructured colloidal liquid crystals found using high-resolution transmission electron microscopy, small-angle X-ray scattering, and neutron scattering and rheological measurements are also reported. The functions of these biomineral-inspired liquid crystals are presented. Because these biomineral-based LC colloidal liquid crystals can be prepared under mild and aqueous conditions and they consist of environmentally friendly and biocompatible components, new functions are expected for these materials.
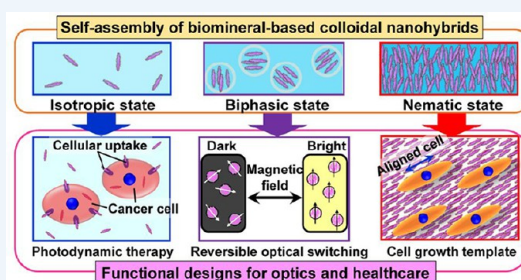
■ KEY REFERENCES

● Nakayama, M.; Kajiyama, S.; Kumamoto, A.; Nishimura, T.; Ikuhara, Y.; Yamato, M.; Kato, T. Stimuli-Responsive Hydroxyapatite Liquid Crystal with Macroscopically Controllable Ordering and Magneto-Optical Functions. *Nat. Commun.* **2018**, 9, 568.[1] Hydroxyapatite-based

nanorod liquid crystals were synthesized using acidic polymers; they demonstrated stimuli-responsive alignment properties. Reversible optical transmission switching was demonstrated under applied magnetic fields.

- Nakayama, M.; Kajiyama, S.; Nishimura, T.; Kato, T. Liquid-Crystalline Calcium Carbonate: Biomimetic Synthesis and Alignment of Nanorod Calcite. *Chem. Sci.* **2015**, 6, 6230−6234.[2] CaCO₃-based nanorods were synthesized through crystallization control using acidic polymers inspired by biomineralization. The anisotropic nanohybrids showed liquid-crystalline behaviors in their concentrated colloidal dispersions and macroscopic alignment in response to an applied mechanical force.

- Nakayama, M.; Lim, W. Q.; Kajiyama, S.; Kumamoto, A.; Ikuhara, Y.; Kato, T.; Zhao, Y. Liquid-Crystalline Hydroxyapatite/Polymer Nanorod Hybrids: Potential Bioplatform for Photodynamic Therapy and Cellular Scaffolds. *ACS Appl. Mater. Interfaces* **2019**, 11, 17759−17765.[3] The biomedical functions of hydroxyapatite-based nanorod liquid crystals were studied. The nanorods with incorporated photosensitizers functioned as drug nanocarriers for photodynamic therapy, and aligned nanorod films were used as cell culture scaffolds to control cell alignment.

1. INTRODUCTION

Liquid crystals are soft materials that combine orientational and/or positional orders and fluidic states. Liquid-crystalline (LC) phases form a wide variety of structural orders through the self-assembly of their components. These anisotropic states include nematic, smectic, cubic, and columnar phases. Some of the most common liquid crystals are molecular-based thermotropic liquid crystals with anisotropic shapes such as rods and disks, which form LC states upon heating. The sizes of the molecules vary from low-molecular-weight compounds to high-molecular-weight polymers.[4−7] Molecular-based liquid crystals exhibiting ordered states with solvents are known as lyotropic liquid crystals. They require appropriate solvents for the induction of mesophases. Lyotropic mesophases are formed by organic compounds, including chromonic and amphiphile molecules, and hydrophilic biomacromolecules with rigid rod shapes, such as DNA and cellulose derivatives (Figure 1a, left).[8,9] Colloidal liquid crystals are another class of materials in which particles are dispersed and aligned in solvents. Colloidal particles comprising viruses, inorganic nanocrystals, inorganic/organic nanohybrids, and nanocrystalline biopolymers have been reported to form LC colloidal phases (Figure 1a, middle).[10−12] The component particles that induce mesophases can be called colloidal mesogens, in comparison with the molecular mesogens found in organic molecular-based liquid crystals.

Figure 1 shows the LC materials that require solvents for the induction of mesophases. Although colloidal particles in the range of 10−1000 nm are relatively large and are insoluble in organic solvents and water, they form LC states in dispersed states, which is different from the induction mechanism for lyotropic LC states typically exhibited by organic molecular surfactants such as hexadecyltrimethylammonium bromide (Figure 1a, left and middle).
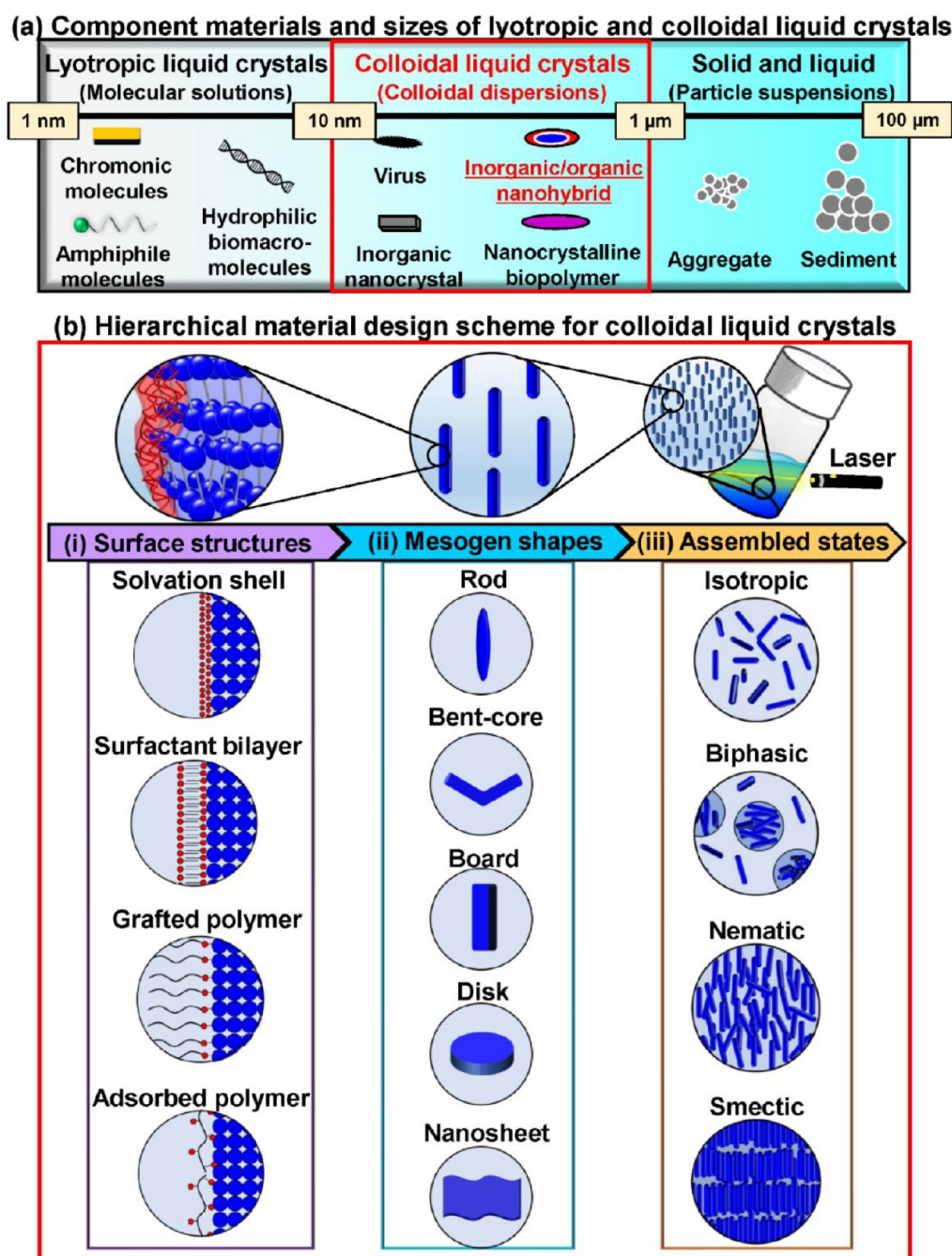
Experimental observations and computer simulations of colloidal mesogens of inorganic nanocrystals have been performed for decades.[13−16] The mesogenic dimensions of

colloidal liquid crystals can give rise to larger structural orders with unique dynamical behaviors and responsive properties under external stimuli, which are clearly distinct from those of their molecular-based counterparts. Thus, even today, LC colloidal fluids can be recognized as an emerging class of self-assembled responsive nanomaterials covering mesoscopic scales. Indeed, novel electric, magnetic, optical, and biological functions have been demonstrated by linking the intrinsic characteristics of colloidal building blocks with self-assembled ordered structures.[1,3,17−23] In spite of their fascinating functions, colloidal liquid crystals are still far less common than molecular-based liquid crystals because of the absence of universally available synthetic processes.

The precise control of the synthesis of anisotropic colloidal particles is indispensable for the further development of colloidal liquid crystals. The use of self-organization processes in aqueous phases is an attractive approach in terms of energy conservation and environmental friendliness. For more than two decades, we have developed inorganic/organic composite materials, including crystalline thin films and bulk solids with finely tuned crystal morphologies, polymorphisms, crystallographic orientations, and nanostructures through self-organization inspired by biomineralization in the presence of acidic proteins and peptides.[24−28] Moreover, we developed colloidal amorphous calcium carbonate (ACC), which is formed from supersaturated solutions of calcium carbonate (CaCO₃) in the presence of poly(acrylic acid) (PAA).[29] Recently, we reported colloidal liquid crystals based on typical inorganic components of biominerals such as CaCO₃ and hydroxyapatite (HAp), which exhibit interesting optical and biomedical functions.[1−3,30] Anisotropic colloidal mesogens with inorganic crystalline cores and organic polymer shells were obtained by crystallizing polymer-stabilized colloidal amorphous precursors. Advanced analytical measurements using transmission electron microscopy (TEM),[1,3] small-angle X-ray scattering (SAXS), X-ray photon correlation spectroscopy (XPCS),[30] and in situ small-angle neutron scattering and rheological measurements (Rheo-SANS)[31] have revealed the nanostructures of the mesogens and dynamic behaviors of the HAp-based liquid crystals. These biomineral-inspired colloidal liquid crystals synthesized under mild conditions can be regarded as a new class of sustainable nanomaterials with self-assembled and stimuli-responsive properties. In this Account, we describe our perspectives on the material design schemes, synthetic methods, and functions of colloidal liquid crystals that combine inorganic and polymer components.

## 2. HIERARCHICAL MATERIAL DESIGN OF BIOMINERAL-INSPIRED COLLOIDAL LIQUID CRYSTALS

For the material design of colloidal liquid crystals, we present a hierarchical scheme with the following factors: (i) functionalized and stabilized surface structures for the mesogens, (ii) anisotropic shapes for individual colloidal mesogens, and (iii) assembled colloidal states (Figure 1b). As exemplified in the literature,[10−12] the self-assembly of anisotropic colloids leads to the formation of LC phases (Figure 1b, (iii)). The most typical phase of colloidal liquid crystals is a nematic phase. The formation of an isotropic/nematic coexisting phase is often observed in a narrow concentration range between the isotropic and nematic phases. For colloidal liquid crystals that exhibit more ordered structures such as smectic and columnar phases, the size and shape polydispersity that inevitably occurs in

(a) Component materials and sizes of lyotropic and colloidal liquid crystals

Lyotropic liquid crystals (Molecular solutions) | **Colloidal liquid crystals** (Colloidal dispersions) | **Solid and liquid** (Particle suspensions)

1 nm — 10 nm — 1 μm — 100 μm

Chromonic molecules

Amphiphile molecules

Hydrophilic biomacro-molecules

Virus

Inorganic nanocrystal

Inorganic/organic nanohybrid

Nanocrystalline biopolymer

Aggregate

Sediment

(b) Hierarchical material design scheme for colloidal liquid crystals

Laser

(i) Surface structures | **(ii) Mesogen shapes** | **(iii) Assembled states**

Surface structures: Solvation shell, Surfactant bilayer, Grafted polymer, Adsorbed polymer

Mesogen shapes: Rod, Bent-core, Board, Disk, Nanosheet

Assembled states: Isotropic, Biphasic, Nematic, Smectic

Figure 1. Material designs and structural hierarchy of colloidal liquid crystals. (a) Materials and sizes for the components of lyotropic liquid crystals, colloidal liquid crystals, and particle suspensions that undergo phase separation into solid and liquid states. (b) Hierarchical material design scheme of colloidal liquid crystals consisting of colloidal mesogens with inorganic rigid cores and organic shells, including the (i) surface structures of the mesogens, (ii) anisotropic mesogen shapes, and (iii) assembled states of the mesogens.

colloidal systems should be reduced during the synthesis and purification processes. The shape anisotropy and rigidity of the colloidal particles, as well as their uniformity, are also important factors that induce LC phases. Previously, rigid anisotropic shapes including rod, bent-core, board, disk, and nanosheet forms as colloidal mesogens were reported (Figure 1b, (ii)).[33−37] The basic mechanism underlying the LC formation by rigid anisotropic particles was formulated based on the Onsager theory.[38] According to this theory, anisotropic mesogens with large aspect ratios show lower critical concentrations for isotropic−LC phase transitions and highly fluidic LC phases with dynamic properties. However, particles

dispersed in solvents often suffer from phase separation into solids and liquids through aggregation and sedimentation without the formation of LC states (Figure 1a, right). Downsizing particles in the range below the micrometer scale could be an effective approach to avoid sedimentation. Electric double layers on particle surfaces also stabilize colloidal dispersions by electrostatic repulsion, which can be achieved by the surface modification of inorganic rigid cores using charged surfactant bilayers or polymer layers as organic shells (Figure 1b, (i)).[39,40] Another way is to sterically hinder the aggregation by surface modification with bulky and dense molecular adsorption layers, including solvation shells and
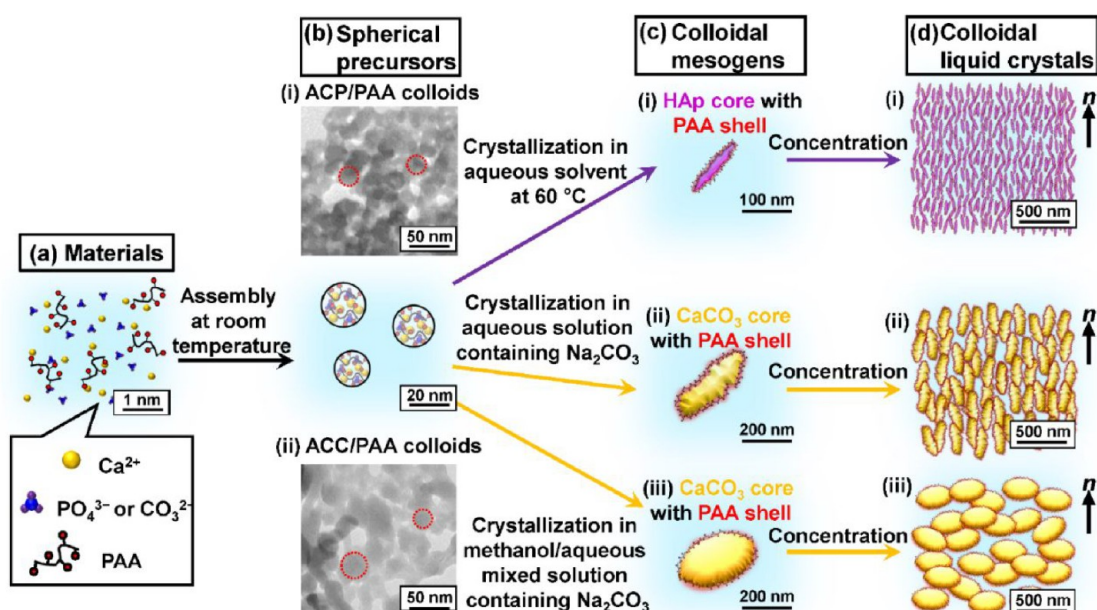
Figure 2. Synthetic processes of biomineral-inspired colloidal liquid crystals combining inorganic and organic components. (a) Inorganic ions interact with PAA to (b) form spherical precursors of (i) ACP/PAA and (ii) ACC/PAA colloids. The graphic (i) in (b): Adapted with permission from ref 1. Copyright (2018) The Authors. The graphic (ii) in (b): Adapted with permission from ref 30. Copyright (2020) Royal Society of Chemistry. (c) Anisotropic colloidal mesogens of (i) HAp nanorods, (ii) CaCO$_3$ nanorods, and (iii) CaCO$_3$ nanodisks are obtained by tuning crystallization conditions for the precursors and (d) form colloidal liquid crystals of (i) HAp nanorods, (ii) CaCO$_3$ nanorods, and (iii) CaCO$_3$ nanodisks through self-assembly by concentration. The arrows denoted by n represent liquid crystal directors.

grafted polymer layers.[41,42] If these kinds of interparticle interactions are greater than the van der Waals attractive forces, the colloidal mesogens maintain dispersed and aligned states without phase separation.

3. SYNTHESIS OF BIOMINERAL-INSPIRED COLLOIDAL LIQUID CRYSTALS

We found that biomineralization-inspired crystallization using acidic polymers could be used as an environmentally friendly and sustainable synthetic approach to prepare colloidal liquid crystals (Figure 2). In biomineralization that occurs in nature, it was proposed that amorphous minerals stabilized by acidic proteins and peptides behave as precursors for the formation of crystalline hard tissues.[27,28,43,44] The intracellular amorphous precursors are transported to the mineralization sites for forming hard tissues, where the amorphous precursors are crystallized in a precisely controlled manner, and nanocrystalline hybrids with desirable morphologies, sizes, polymorphs, and crystallographic orientations are produced.[45−48] Recent studies revealed that the crystal growth processes are based on nonclassical crystallization through colloidal amorphous precursors, which is distinguished from classical crystallization by the ion-by-ion attachment.[49−51] Although it is difficult to clarify the crystallization mechanism in vivo, the transformation of amorphous precursors into crystalline states has been examined in synthetic systems as a new approach to develop functional crystalline hybrid materials. In relation to biomineralization, our group intensively explored the use of PAA as an acidic macromolecular additive to inhibit the direct crystallization of CaCO$_3$ or HAp and stabilize ACC and amorphous calcium phosphate (ACP).[29,52] In the presence of PAA, Ca^{2+} interacts with the carboxylate groups of PAA, in addition to counter inorganic ions such as CO$_3{}^{2-}$ or PO$_4{}^{3-}$ (Figure 2a), to from spherical amorphous assemblies, which are available as colloidal precursors (Figure 2b). The amorphous precursors are transformed into anisotropic crystalline nano-hybrids by tuning the crystallization conditions (Figure 2c). PAA also plays key roles in the surface modification of inorganic cores based on CaCO$_3$ and HAp as well as in the morphological control.[53−55] Tuning the PAA concentration is important to stabilize the amorphous precursors in the supersaturated solutions and to control the crystallization and the crystal growth. The concentrations of inorganic ions such as Ca^{2+} and CO$_3{}^{2-}$ or PO$_4{}^{3-}$ as well as the monomer units of PAA were adjusted to be 50 mM in the mixed solution. The lower PAA concentrations increase the crystallization rates, resulting in the increase of particle sizes and the decrease of the shape anisotropy. The amounts of the PAA on the surface were also decreased to destabilize the colloidal states. The higher PAA concentrations decrease the yields of the amorphous precursors due to the decrease of pH values of the solutions. HAp-based nanorods covered with PAA shells (Figure 2c, (i)) were obtained from colloidal ACP/PAA precursors (Figure 2b, (i)) by heating aqueous dispersions up to 60 °C.[1] In the case of ACC/PAA (Figure 2b, (ii)), the amorphous precursors were transformed into CaCO$_3$-based nanorods with surface PAA shells (Figure 2c, (ii)) in an aqueous solution containing Na$_2$CO$_3$ as a crystallization accelerator.[2] In contrast, CaCO$_3$-based nanodisks with PAA shells were obtained in a methanol/water mixed solvent containing Na$_2$CO$_3$ at room temperature (Figure 2c, (iii)).[30] These different shapes for HAp or CaCO$_3$-based colloids formed LC states by concentration-driven self-assembly (Figure 2d). The increase of the particle concentrations in the solvents over the phase transition concentrations through evaporation or centrifugation processes led to the spontaneous formation of nematic structures with random domains. Furthermore, the degree and the direction of orientation can be macroscopically controlled by applying
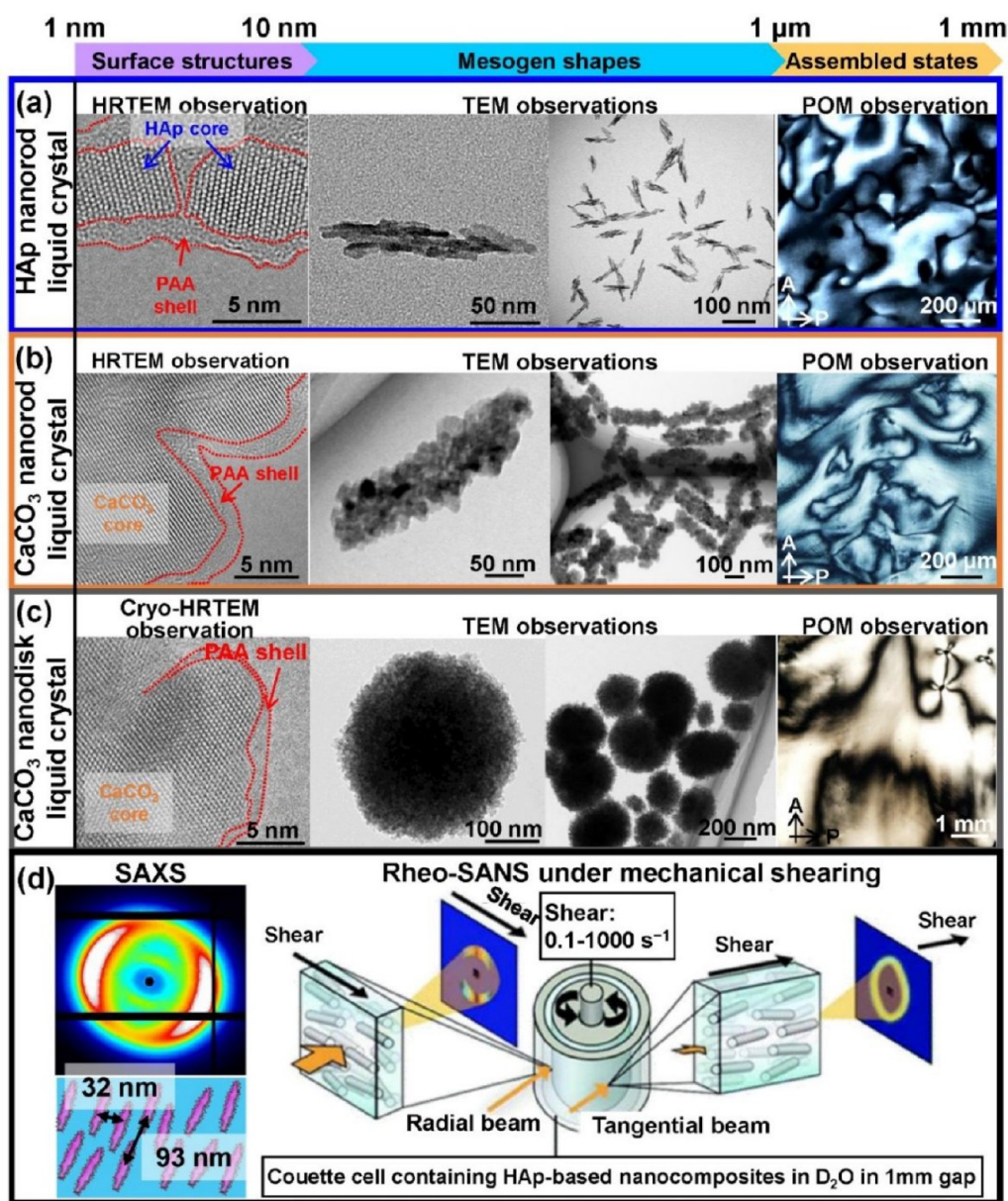
Figure 3. Material characterizations of biomineral-inspired colloidal liquid crystals composed of inorganic cores and organic shells. (a−c) HRTEM observations, conventional TEM observations, and POM observations of (a) a HAp nanorod liquid crystal, (b) CaCO$_3$ nanorod liquid crystal, and (c) CaCO$_3$ nanodisk liquid crystal. A: Analyzer. P: Polarizer. The panel (a): Adapted with permission from ref 1. Copyright (2018) The Authors. The TEM images in (b): Adapted with permission from ref 30. Copyright (2020) Royal Society of Chemistry. The POM image in (b): Adapted with permission from ref 2. Copyright (2015) Royal Society of Chemistry. The panel (c): Adapted with permission from ref 30. Copyright (2020) Royal Society of Chemistry. (d) Structural analyses of a nematic phase of a HAp liquid crystal using SAXS and Rheo-SANS. The SAXS graphic in (d): Adapted with permission from ref 31. Copyright (2019) Royal Society of Chemistry. The Rheo-SANS graphic in (d): Adapted with permission from ref 32. Copyright (2020) Royal Society of Chemistry.

magnetic fields using superconducting magnets and by applying mechanical stresses using shearing or spin-coating machines.

4. CHARACTERIZATIONS OF BIOMINERAL-INSPIRED COLLOIDAL LIQUID CRYSTALS

The distinct mesogens of HAp nanorods, CaCO$_3$ nanorods, and nanodisks were characterized using various advanced analytical techniques (Figure 3). The Schlieren textures observed by polarizing optical microscopy (POM) after concentration indicated the formation of nematic phases for these colloidal liquid crystals (Figure 3a−c, right). To obtain further insights into the LC properties, the anisotropic morphologies and

functionalized surfaces of these mesogens were observed using conventional TEM, aberration-corrected high-resolution TEM (HRTEM), and cryogenic HRTEM (cryo-HRTEM) (Figure 3a−c, left and middle). The HAp-based mesogens displayed nanorod shapes with average lengths and widths of 100 ± 20 nm and 21 ± 5 nm, respectively (Figure 3a, middle). The aspect ratio of the nanorods was 5.0. The atomic columns corresponding to the HAp crystals with the zone axis of [320] were observed for the inorganic core composed of rod-shaped nanocrystallites (Figure 3a, left). The experimentally observed atomic-scale images were in good agreement with the simulation results. The nanocrystallites were connected by amorphous PAA
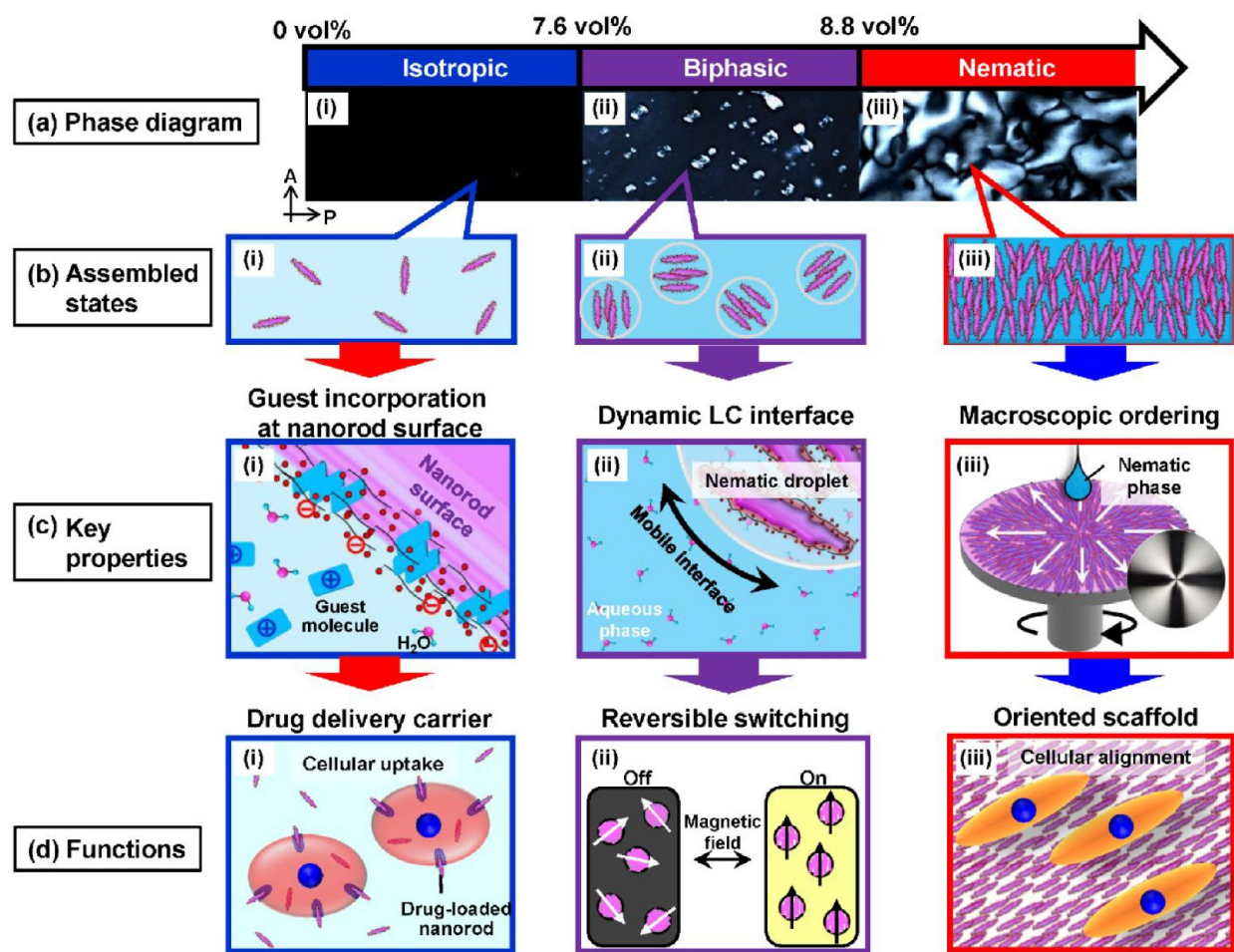
Figure 4. Functional designs of the HAp nanorod liquid crystal in each phase. (a) Phase diagram of the HAp liquid crystal showing (i) isotropic, (ii) isotropic/nematic coexisting, and (iii) nematic phases. Schematic illustrations of (b) assembled colloidal states, (c) key properties, and (d) functions of (i) isotropic, (ii) isotropic/nematic coexisting, and (iii) nematic phases.

domains, and the nanorod surfaces were also covered with 1−2 nm thick PAA shells, contributing to negative zeta potentials of −39 ± 7 mV on the nanorod surfaces. The self-assembled behavior of the HAp nanorod mesogens was further revealed using SAXS, XPCS, and Rheo-SANS.[31,32] In the SAXS measurements, the LC phase at 8.7 vol % showed a nematic structure with interparticle distances of 93 and 32 nm in the long- and short-axis directions of the nanorods, respectively (Figure 3d, left). In addition, anisotropic dynamics with a faster relaxation rate in the long-axis direction were observed for the nematic phase using XPCS. In the oriented state, the directional anisotropy of the diffusion constant increases depending on the particle aspect ratio, which can be derived from the theoretical formula for the friction coefficients of the rod-shaped particles.[56] Rheo-SANS measurements revealed a shear-induced transition from a nematic to a smectic-like structure (Figure 3d, right). For the CaCO_3 nanorod liquid crystal, the mesogens were estimated to be 300 ± 78 nm in length and 97 ± 24 nm in width (Figure 3b, middle), and the aspect ratios were 3.1 ± 0.4. The rigid inorganic cores of the nanorods were composed of connected nanocrystallites with sizes of approximately 20 nm (Figure 3b, left). Atomic-scale HRTEM observations showed lattice fringes corresponding to the (006) plane of calcite crystals. The surfaces of the inorganic cores were covered with organic shells of PAA with a thickness of approximately 1−2 nm, leading to

negative zeta potentials of −14.7 ± 6 mV on the nanorod surfaces. For the CaCO_3 nanodisk liquid crystals, the average diameters of the mesogens were estimated to be 320 ± 74 nm from the TEM images (Figure 3c, middle), and the thicknesses were 137 ± 80 nm according to atomic force microscopy observations. Therefore, the aspect ratio of the nanodisks was estimated to be approximately 2.5. The crossed lattice fringes of vaterite crystals were clearly observed by cryo-HRTEM techniques to suppress the electron irradiation damage for the unstable vaterite crystals. The rigid inorganic core was covered with an amorphous PAA shell with a thickness of approximately 1−2 nm (Figure 3c, left), which generated negative zeta potentials of −17.4 ± 6 mV on the nanodisk surfaces.

5. FUNCTIONAL DESIGNS OF BIOMINERAL-INSPIRED COLLOIDAL LIQUID CRYSTALS

Their aqueous-based mild synthetic processes and biofriendly components make exploring the applications of biomineral-inspired liquid crystals an attractive challenge. These liquid crystals can be functionalized by combining the properties of colloidal mesogens and their dynamic self-assembled structures. We have pursued the functionalization of the HAp liquid crystal as a potential platform for various applications, taking advantage of the biomedical properties of HAp, host−guest interactions at the PAA shells, optical transparency and long-term colloidal
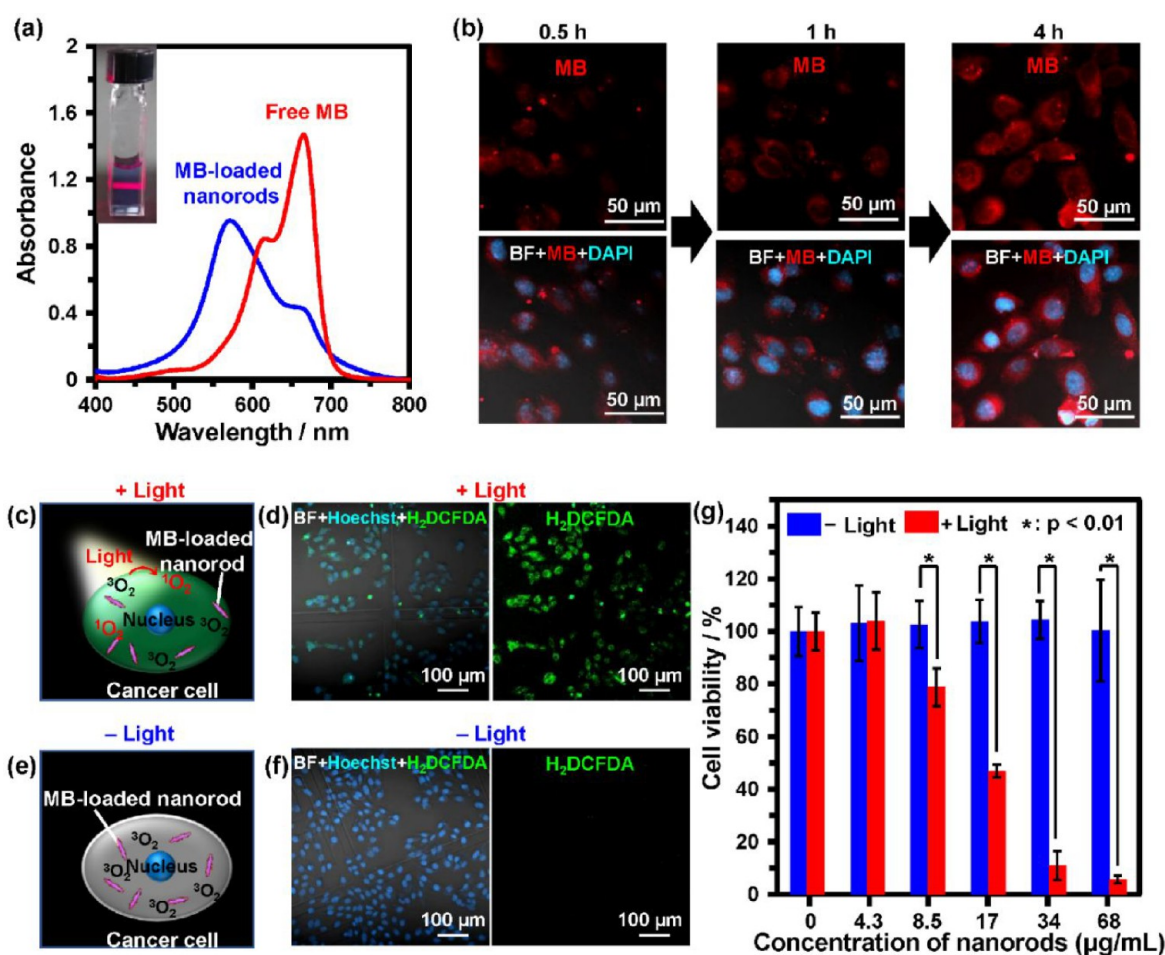
Figure 5. Functionalization of the isotropic phase of the HAp liquid crystal for PDT drug nanocarriers. (a) Absorbance spectra of an isotropic colloidal dispersion of MB-loaded HAp nanorods and free MB solution. The inset shows a digital photograph of an isotropic colloidal dispersion of MB-loaded nanorods displaying a blue color and Tyndall scattering. (b) Time-dependent cellular uptake of MB-loaded nanorods (68 μg/mL) observed by CLSM, where MB shows red fluorescence, and the cell nuclei stained by DAPI display blue fluorescence. (c,e) Schematic illustrations of (c) a cancer cell with cytotoxic $^1O_2$ generated by intracellular MB-loaded nanorods under light irradiation and (e) a cancer cell without cytotoxic $^1O_2$ but with intracellular MB-loaded nanorods in the absence of light irradiation. (d,f) CLSM images of HeLa cells (d) incubated in isotropic colloidal dispersions of MB-loaded nanorods (17 μg/mL) for 4 h and then irradiated with light (100 mW/cm^2) for 10 min and (f) incubated under the same conditions without light irradiation. The cell nuclei stained with Hoechst 33342 show blue fluorescence. H$_2$DCFDA oxidized by $^1O_2$ shows green fluorescence. (g) Cell viabilities of HeLa cells incubated with different concentrations of MB-loaded nanorods for 24 h with or without light irradiation. Bright field images in (b,d,f) are designated by BF. The panels (a–g): Adapted with permission from ref 3. Copyright (2019) American Chemical Society.

stability in the colloidal states, and stimuli-responsive structural changes in the LC self-assembled states. With an increase in the concentration, the HAp nanorods initially underwent phase transitions from an entirely isotropic (Figure 4a, (i)) to an isotropic/nematic coexisting biphasic state at 7.6 vol % (Figure 4a, (ii)) and finally reached a homogeneous nematic phase at 8.8 vol % (Figure 4a, (iii)). Based on the concentration-dependent LC properties, we designed functions reflecting the self-assembled states for each of the phases (Figure 4b–d). HAp liquid crystals can be used as nanocarriers for drug delivery in the isotropic state (Figure 4d, (i)),[3] reversible optical switching systems in the biphasic state (Figure 4d, (ii)),[1] and cell culture scaffolds in the nematic state (Figure 4d, (iii)).[3]

In the isotropic phase, a diluted colloidal dispersion of nanorods has no orientational order (Figure 4b, (i)), but a single colloidal mesogen component with a negatively charged organic polymer shell has the capability to incorporate guest molecules with positive charges (Figure 4c, (i)). For example, methylene blue (MB), which is a photosensitizer available for photo-dynamic cancer therapy,[57,58] can be introduced into the PAA

shells (Figure 3a, left). The colloidal stability and biocompatibility of the mesogens are also advantageous for delivering loaded drugs to tumor sites, and the shape anisotropy can be beneficial for efficient cellular uptake (Figure 4d, (i)).[59]

In the biphasic state, phase-separated nematic droplets exist in the isotropic phase without a specific orientation (Figure 4b, (ii)), but the orientations of nematic droplets can be remotely manipulated using external magnetic fields because of the diamagnetic anisotropy of HAp.[60] The nematic domains have a mobile interface with the surrounding aqueous medium (Figure 4c, (ii)), in contrast to the nematic phase being in touch with the solid surfaces of device cells, which induces strong anchoring interactions. Furthermore, biphasic dispersions are optically transparent, because the HAp nanorods show neither light absorption nor scattering in the visible wavelength range. Based on these magnetic and optical properties, we used biphasic states as a reversible magneto-optical switching system (Figure 4d, (ii)).

The single nematic phase can be used to obtain solid films with stable macroscopic alignment of the nanorod particles by
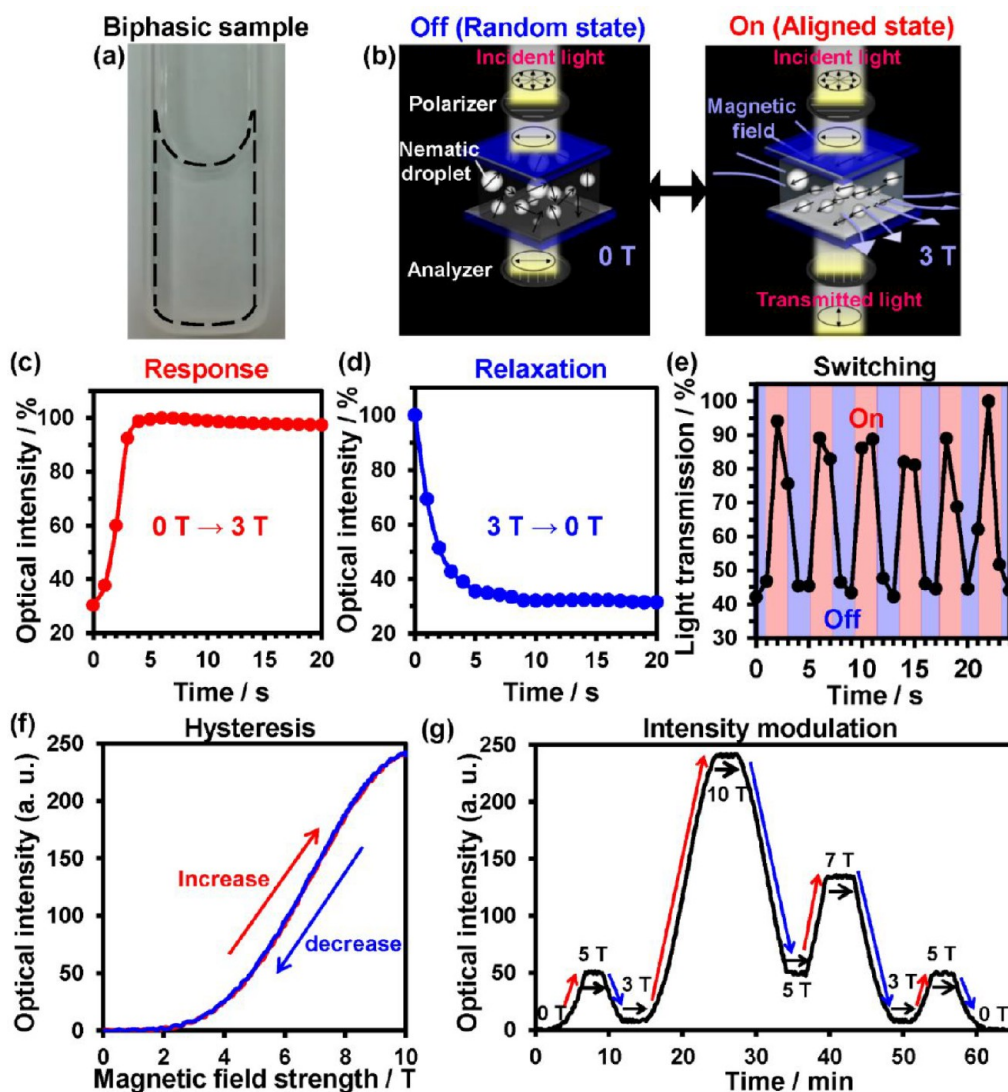
Figure 6. Functionalization of the isotropic/nematic coexisting phase of the HAp liquid crystal for a magneto-optical switching system. (a) Digital photograph of a biphasic colloidal dispersion of HAp nanorods at 8.5 vol % in a 2 mm thick optical cell. (b) Schematic illustration of nematic droplets in a biphasic state, which shows light transmission and insulation under crossed polarizers in the presence (left) and absence (right) of a magnetic field of 3 T, respectively. (c) Optical response behavior in a biphasic state by application of a magnetic field of 3 T. (d) Optical relaxation behavior in a biphasic state by removal of a magnetic field of 3 T. (e) Changes with time of the transmitted light intensity in a biphasic state when the magnetic field of 3 T was repeatedly turned on and off. (f) Change in the intensity of light transmission through a biphasic state, while magnetic field was increased from 0 to 10 T and decreased from 10 to 0 T. (g) Modulation of light transmission through a biphasic state by tuning the strength of the applied magnetic field. The panels (a−g): Adapted with permission from ref 1. Copyright (2018) The Authors.

mechanical stimuli such as rubbing and spin-coating (Figure 4b, (iii)). The oriented structures are easily preserved by evaporating the aqueous solvent because of the higher concentration and slower dynamics of the colloidal mesogen particles (Figure 4c, (iii)). Taking advantage of the biocompatibility of HAp, the anisotropic coating can be applied to cell culture scaffolds to control cell growth, alignment, and morphology for tissue engineering (Figure 4d, (iii)).

6. FUNCTIONALIZATION OF THE ISOTROPIC PHASE OF THE HAP LIQUID CRYSTAL FOR DRUG NANOCARRIERS

The nanorod mesogens in the isotropic phases have biocompatibility, colloidal stability, and drug loading and pH-responsive release ability, which can be useful for drug delivery to tumor sites and cancer therapy. We used a single colloidal

mesogen component in the isotropic phase of the HAp liquid crystal as a drug nanocarrier for photodynamic therapy (PDT),[3] while Liu and Fan used randomly dispersed colloidal $CaCO_3$ nanorods prepared by our methods for tumor therapy, PDT, and ultrasound bioimaging.[61,62] In our approach, MB was selected as a molecular model drug that generates singlet oxygen ($^1O_2$) under light excitation and kills cancer cells through oxidative stresses. HAp nanorods with MB molecules incorporated in the PAA shell region through electrostatic interactions showed absorbance peaks at 570 nm, which reflected a blue-shift from the absorbance at 665 nm for free MB (Figure 5a). This observation suggested that the MB molecules were highly condensed on the nanorod surfaces to form H-aggregates. The amount of MB loaded in the hybrid nanorods was estimated to be 3.6 wt % based on the absorbance spectra and thermogravimetric analyses. Photobleaching and enzymatic reduction were suppressed for the loaded MB compared to
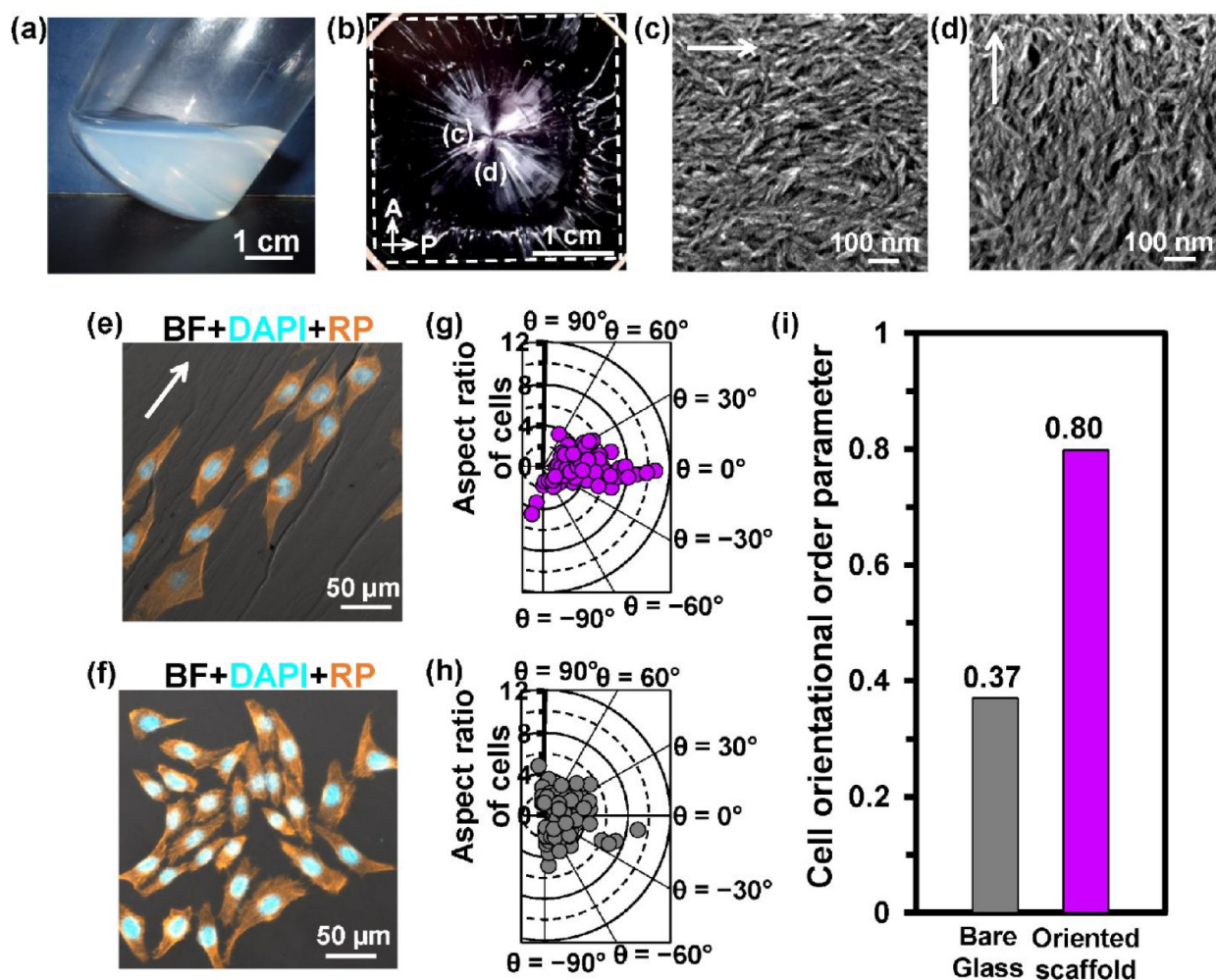
Figure 7. Functionalization of the nematic phase of the HAp liquid crystal for oriented scaffolds. (a) Digital photograph of a nematic colloidal dispersion of HAp nanorods at 9.2 vol % in a sample bottle. (b) POM image of radially oriented nanorod assemblies prepared as an oriented scaffold by spin-coating a nematic colloidal dispersion. A: Analyzer. P: Polarizer. (c,d) SEM images of the regions on the surface of the oriented scaffold denoted by (c) and (d) in (b), respectively. The white arrows represent the alignment directions of the HAp nanorods. (e,f) CLSM images of cells cultured on (e) an oriented scaffold and (f) a bare glass substrate. Actin fibers stained with RP show orange fluorescence, and cell nuclei stained with DAPI show blue fluorescence. The white arrow in (e) indicates the alignment direction of the HAp nanorods. (g,h) Polar plots of the aspect ratios and orientation angles of cells cultured on (g) oriented scaffolds and (h) bare glass substrates. (i) Orientational order parameters of cells cultured on oriented scaffolds and bare glass substrates. The bright field images in (e) and (f) are designated by BF. The panels (a–i): Adapted with permission from ref 3. Copyright (2019) American Chemical Society.

free MB, which suggested that the PAA shells increased the lifetime as a PDT agent. The cellular accumulation ability of the MB-loaded nanorods was confirmed by observing the time-dependent increase in red fluorescence arising from MB molecules within human cervical carcinoma (HeLa) cells using confocal laser scanning microscopy (CLSM) (Figure 5b). The nuclei of the HeLa cells were stained with 4′,6-diamidino-2-phenylindole (DAPI) to display blue fluorescence. These observations suggested that the nanorods were internalized into the cells with increasing time, whereas no cellular uptake was observed for free MB molecules. The ability to generate $^1O_2$ was examined for intracellular MB-loaded nanorods. The cell nuclei were stained with Hoechst 33342, and the generated $^1O_2$ was visualized using 2′,7′-dichlorodihydro-fluorescein diacetate (H_2DCFDA), which emits green fluo-rescence after a reaction with $^1O_2$. The MB-loaded nanorods within the cells worked well as photosensitizers for the generation of $^1O_2$ under light irradiation (Figure 5c,d). In contrast, negligible green fluorescence was observed without

light irradiation (Figure 5e,f). Finally, the cell photocytotoxicity was investigated using a 3-(4,5-dimethylthiazol-2-yl)-2,5-diphenyltetrazolium bromide (MTT) assay (Figure 5g). Under dark conditions, no cytotoxicity was observed, suggesting the high biocompatibility of the MB-loaded nanorod carriers. In contrast, cell viability decreased to 5% after light irradiation at a concentration of 68 μg/mL. The MB-loaded nanorods showed a high cellular uptake, biocompatibility, and an efficient cancer cell killing ability under light irradiation, demonstrating their potential as nanocarriers for PDT.

For $CaCO_3$ nanorods, colloidal mesogens were used as pH-responsive components in the drug carrier for shape switching.[61] Liu et al. used rod-shaped morphologies to prolong the blood circulation time and enhance extravasation into tumor tissues. The carriers obtained sphere-like morphologies by the removal of the $CaCO_3$ nanorods in response to an acidic tumor, leading to the promotion of tumor cell uptake, followed by the intracellular release of chemotherapeutic agents.

7. FUNCTIONALIZATION OF THE ISOTROPIC/NEMATIC COEXISTING PHASE OF THE HAP LIQUID CRYSTAL FOR A REVERSIBLE MAGNETO-OPTICAL SWITCHING SYSTEM

The isotropic/nematic coexisting phase is advantageous for magneto-optic modulation, because the phase-separated nematic droplets show faster orientation behaviors in response to applied magnetic fields compared with the homogeneous nematic state with anchoring effects on the solid surfaces of the device cell. In the biphasic state with the mobile LC interfaces and high optical transparency (Figure 6a), the optical transmission switching properties were demonstrated by measuring changes in the transmitted light intensity upon the application of magnetic fields under crossed polarizers (Figure 6b).[1] Nematic droplets with a diameter of a few micrometers were phase-separated from the isotropic phase. They were randomly oriented in an aqueous medium, resulting in low light transmission under crossed polarizers in the absence of magnetic fields. The biphasic states reached the maximum brightness within a few seconds in response to an applied magnetic field of 3 T (Figure 6c). The increase in brightness resulted from the uniform orientation of the nematic droplets. When the magnetic field was turned off, relaxation started immediately, and the system returned to the initial low value of brightness within a few seconds (Figure 6d). This dynamic behavior allowed rapid oscillations of the transmitted light intensity within a few seconds when the magnetic field of 3 T was alternately turned on and off (Figure 6e). Magnetic modulation of the transmission intensity was also achieved without hysteresis by tuning the magnetic field strength applied to the biphasic system (Figure 6f). The light transmission intensity of the biphasic system precisely followed the changes in the strength of the external magnetic field, as shown in Figure 6g. Light transmission was 27 times higher at 10 than at 3 T, showing a large contrast ratio and application potential for optical switching and modulation systems. This is because the anisotropic magnetic energy is proportional to the square of the magnetic field strength, and the orientational behaviors of nematic droplets do not suffer from anchoring effects at the LC interfaces.

Wang et al. also reported magnetically actuated colloidal liquid crystals based on Fe_3O_4 nanorods, which are highly sensitive to a directional change in an external magnetic field.[63] In the liquid crystal film, magnetically aligned Fe_3O_4 nanorods led to the creation of patterns of different polarizations and control over the transmittance of light in particular areas.

8. FUNCTIONALIZATION OF THE NEMATIC PHASE OF THE HAP LIQUID CRYSTAL FOR ANISOTROPIC CELL CULTURE SCAFFOLDS

We demonstrated the potential of the nematic phase of the HAp liquid crystal (Figure 7a) as a biotemplate to control cell growth to enhance cell differentiation and function in tissue engineering.[3] HAp is one of the most useful inorganic biomaterials for cell culture scaffolds because of its biomedical properties,[64] and adjusting the macroscopic orientation could make it possible to control the adhesion, growth, morphology, and alignment of cells.[65−67] It is assumed that the cultured cells sense the anisotropically patterned surfaces of the scaffolds by morphologically reorganizing the cytoskeleton along the aligned direction.[66] Thus, the biomineral-based films with oriented structures are expected to work as cell culture scaffolds for cellular alignment and growth templates. Our approach was to use the self-assembly of liquid crystals for the preparation of macroscopically oriented HAp-based bioscaffolds. Such scaffolds were fabricated by spin-coating HAp liquid crystals on a glass substrate covered with poly(vinyl alcohol) as a binder, and the oriented structures were strongly fixed even after being washed with water or soaked in cell culture medium (Figure 7b–d). In scanning electron microscopy (SEM) images, the HAp nanorods were aligned from the center toward the periphery of the substrate (Figure 7c,d). HeLa cells were cultured on oriented scaffolds prepared from HAp liquid crystals and a bare glass substrate as a control. The cell cytoplasm was stained with rhodamine phalloidin (RP), and the cell nuclei were stained with DAPI. CLSM observations clearly showed that the cells adhered to the surface of the nanorod assembly and aligned along the oriented direction of the HAp nanorods (Figure 7e). In contrast, no cellular alignment was observed for the bare glass substrate (Figure 7f). Figure 7g,h shows polar plots as functions of the aspect ratio and growth angle for cells cultured on oriented scaffolds and bare glass substrates, respectively. The orientational order parameter of the cells (S) was estimated according to the following equation

$$S = \frac{<3\cos^2\theta - 1>}{2}$$

where θ is the orientation angle of the cell. The cells cultured on the oriented scaffolds showed an orientational order parameter of 0.80, which was twice that of cells cultured on a bare glass substrate (Figure 7i). These results suggest that the cultured cells recognized the aligned directions of HAp nanorods on the scaffold surface. Although other reported scaffolds based on aligned synthetic materials including polymeric nanofibers and LC elastomers can also control cell growth,[65−67] our approach can partially resemble the structures, mechanical properties, and chemical compositions of biological hard tissues, which should be more useful for the regenerative tissue engineering.

9. CONCLUSION AND FUTURE OUTLOOK

We describe our design and function for new colloidal liquid crystals based on the anisotropic shapes of biominerals with surface modification. They act as colloidal mesogens, because they are individual nanoparticles and form macroscopically self-assembled colloidal states. Biomineralization-inspired crystallization utilizing acidic polymers has enabled the development of anisotropic inorganic mesogens covered with polymer shells. In these structural formations, PAA plays a significant role in the morphological control and surface modification of $CaCO_3$ and HAp. Several types of structural orders, including isotropic, isotropic/nematic biphasic, nematic, and smectic states, were obtained depending on the particle concentration and external environment.[1,30,31] The liquid crystals exhibited biological and optical functions for drug protection and delivery in the isotropic dispersed state, reversible magneto-optical switching and modulation in the biphasic state, and cellular growth and alignment templates in the nematic state. In functional design, it is very important to find synergistic functions by combining various factors of colloidal liquid crystals, including the chemical properties of the inorganic cores and organic shells, shapes and nanostructures of the colloidal mesogens, and LC assembled structures as well as the dynamical alignment behaviors. Such functionalization approaches would lead to new applications in interdisciplinary fields that are unachievable with conventional molecular-based liquid crystals.

The next challenge for the further advancement of colloidal liquid crystals is to develop a universal synthetic methodology for colloidal LC nanomaterials with desired shapes, similar to the organic synthetic techniques used to design molecular-based liquid crystals. The use of computer simulations and analytical technologies will deepen the molecular-level understanding of multiple noncovalent interactions between organic and inorganic compounds in solution states, which may enable the rational design of a variety of anisotropic nanohybrids. Strategic design of molecular components to control the inorganic crystallization is also of great importance. The further identification of natural proteins and peptides[27,28] involved in the biomineralization will provide further insights into the design of functional groups, sequences, and molecular weights of synthetic organic additives.

Another challenge is to obtain highly aligned and hierarchical structures comparable to those of biological composites. Such hierarchically aligned structures could be achieved by the development of methodologies for spatiotemporally controlled processing of biomineral-based colloidal liquid crystals. In addition, helical, honeycomb, or foam-like porous materials can be constructed as complex templates with advanced printing and molding technology. For composite formation, colloidal LC biominerals can be incorporated into the materials. This approach could provide a way to develop novel high-strength composite materials with well-organized hierarchical structures resembling biominerals.

The material designs and applications of colloidal liquid crystals using biofriendly resources and processes may provide valuable insights in the field of sustainable self-assembled nanomaterials, which could be useful for solving the ever-increasing global problems associated with the environment, energy, and healthcare.

■ AUTHOR INFORMATION

Corresponding Authors

Masanari Nakayama − *Department of Chemistry & Biotechnology, School of Engineering, The University of Tokyo, Tokyo 113-8656, Japan;* ○ orcid.org/0000-0001-7023-3801; Email: masanarinakayama@gmail.com

Takashi Kato − *Department of Chemistry & Biotechnology, School of Engineering, The University of Tokyo, Tokyo 113-8656, Japan; Research Initiative for Supra-Materials, Shinshu University, Wakasato, Nagano 380-8553, Japan;* ○ orcid.org/0000-0002-0571-0883; Email: kato@chiral.t.u-tokyo.ac.jp

Complete contact information is available at:
https://pubs.acs.org/10.1021/acs.accounts.2c00063

Notes

The authors declare no competing financial interest.

Biographies

Masanari Nakayama received his Ph.D. degree from the University of Tokyo under the supervision of Prof. Takashi Kato in 2019 and currently works in the chemical industry as a research scientist. His research interests include functional plastics and metamaterials.

Takashi Kato received his B.S. and Ph.D. degrees from the University of Tokyo in 1983 and 1988, respectively. He was a postdoctoral fellow at Cornell University from 1988 to 1989. He then joined the University of Tokyo as a faculty member. He is currently a professor at the

University of Tokyo. He has also been a professor (cross-appointment) at Shinshu University since 2021. His research interests include the development and functionalization of liquid crystals, polymers, and organic/inorganic materials based on self-organization and supramolecular approaches.

■ ACKNOWLEDGMENTS

■ REFERENCES

(1) Nakayama, M.; Kajiyama, S.; Kumamoto, A.; Nishimura, T.; Ikuhara, Y.; Yamato, M.; Kato, T. Stimuli-Responsive Hydroxyapatite Liquid Crystal with Macroscopically Controllable Ordering and Magneto-Optical Functions. *Nat. Commun.* **2018**, *9*, 568.

(2) Nakayama, M.; Kajiyama, S.; Nishimura, T.; Kato, T. Liquid-Crystalline Calcium Carbonate: Biomimetic Synthesis and Alignment of Nanorod Calcite. *Chem. Sci.* **2015**, *6*, 6230−6234.

(3) Nakayama, M.; Lim, W. Q.; Kajiyama, S.; Kumamoto, A.; Ikuhara, Y.; Kato, T.; Zhao, Y. Liquid-Crystalline Hydroxyapatite/Polymer Nanorod Hybrids: Potential Bioplatform for Photodynamic Therapy and Cellular Scaffolds. *ACS Appl. Mater. Interfaces* **2019**, *11*, 17759−17765.

(4) Kato, T.; Uchida, J.; Ichikawa, T.; Sakamoto, T. Functional Liquid Crystals towards the Next Generation of Materials. *Angew. Chem., Int. Ed.* **2018**, *57*, 4355−4371.

(5) Kato, T.; Yoshio, M.; Ichikawa, T.; Soberats, B.; Ohno, H.; Funahashi, M. Transport of Ions and Electrons in Nanostructured Liquid Crystals. *Nat. Rev. Mater.* **2017**, *2*, 17001.

(6) Bremer, M.; Kirsch, P.; Klasen-Memmer, M.; Tarumi, K. The TV in Your Pocket: Development of Liquid-Crystal Materials for the New Millennium. *Angew. Chem., Int. Ed.* **2013**, *52*, 8880−8896.

(7) Fleischmann, E. K.; Zentel, R. Liquid-Crystalline Ordering as a Concept in Materials Science: From Semiconductors to Stimuli-Responsive Devices. *Angew. Chem., Int. Ed.* **2013**, *52*, 8810−8827.

(8) Van't Hag, L.; Gras, S. L.; Conn, C. E.; Drummond, C. J. Lyotropic Liquid Crystal Engineering Moving beyond Binary Compositional Space-Ordered Nanostructured Amphiphile Self-Assembly Materials by Design. *Chem. Soc. Rev.* **2017**, *46*, 2705−2731.

(9) Fong, C.; Le, T.; Drummond, C. J. Lyotropic Liquid Crystal Engineering-Ordered Nanostructured Small Molecule Amphiphile Self-Assembly Materials by Design. *Chem. Soc. Rev.* **2012**, *41*, 1297−1322.

(10) Lekkerkerker, H. N. W.; Vroege, G. J. Liquid Crystal Phase Transitions in Suspensions of Mineral Colloids: New Life from Old Roots. *Phil. Trans. R. Soc. A.* **2013**, *371*, 20120263.

(11) Davidson, P.; Gabriel, J. C. P. Mineral Liquid Crystals. *Curr. Opin. Colloid Interface Sci.* **2005**, *9*, 377−383.

(12) Sonin, A. S. Inorganic Lyotropic Liquid Crystals. *J. Mater. Chem.* **1998**, *8*, 2557−2574.

(13) Paineau, E.; Krapf, M. E. M.; Amara, M. S.; Matskova, N. V.; Dozov, I.; Rouzière, S.; Thill, A.; Launois, P.; Davidson, P. A Liquid-Crystalline Hexagonal Columnar Phase in Highly-Dilute Suspensions of Imogolite Nanotubes. *Nat. Commun.* **2016**, *7*, 10271.

(14) Van Der Kooij, F. M.; Kassapidou, K.; Lekkerkerker, H. N. W. Liquid Crystal Phase Transitions in Suspensions of Polydisperse Plate-like Particles. *Nature* **2000**, *406*, 868−871.

(15) Veerman, J. A. C.; Frenkel, D. Phase Behavior of Disklike Hard-Core Mesogens. *Phys. Rev.* **1992**, *45*, 5632−5648.

(16) Bolhuis, P.; Frenkel, D. Tracing the Phase Boundaries of Hard Spherocylinders. *J. Chem. Phys.* **1997**, *106*, 666−687.

(17) Lan, T.; Ding, B.; Huang, Z.; Bian, F.; Pan, Y.; Cheng, H. M.; Liu, B. Collective Behavior Induced Highly Sensitive Magneto-Optic Effect in 2D Inorganic Liquid Crystals. *J. Am. Chem. Soc.* **2021**, *143*, 12886−12893.

(18) Zeng, M.; King, D.; Huang, D.; Do, C.; Wang, L.; Chen, M.; Lei, S.; Lin, P.; Chen, Y.; Cheng, Z. Iridescence in Nematics: Photonic Liquid Crystals of Nanoplates in Absence of Long-Range Periodicity. *Proc. Natl. Acad. Sci. U. S. A.* **2019**, *116*, 18322−18327.

(19) Xia, Y.; Mathis, T. S.; Zhao, M. Q.; Anasori, B.; Dang, A.; Zhou, Z.; Cho, H.; Gogotsi, Y.; Yang, S. Thickness-Independent Capacitance of Vertically Aligned Liquid-Crystalline MXenes. *Nature* **2018**, *557*, 409−412.

(20) Kim, J.; Michelin, S.; Hilbers, M.; Martinelli, L.; Chaudan, E.; Amselem, G.; Fradet, E.; Boilot, J. P.; Brouwer, A. M.; Baroud, C. N.; Peretti, J.; Gacoin, T. Monitoring the Orientation of Rare-Earth-Doped Nanorods for Flow Shear Tomography. *Nat. Nanotechnol.* **2017**, *12*, 914−919.

(21) Wong, M.; Ishige, R.; White, K. L.; Li, P.; Kim, D.; Krishnamoorti, R.; Gunther, R.; Higuchi, T.; Jinnai, H.; Takahara, A.; Nishimura, R.; Sue, H.-J. Large-Scale Self-Assembled Zirconium Phosphate Smectic Layers via a Simple Spray-Coating Process. *Nat. Commun.* **2014**, *5*, 3589.

(22) Fu, M.; Chaudhary, K.; Lange, J. G.; Kim, H. S.; Juarez, J. J.; Lewis, J. A.; Braun, P. V. Anisotropic Colloidal Templating of 3D Ceramic, Semiconducting, Metallic, and Polymeric Architectures. *Adv. Mater.* **2014**, *26*, 1740−1745.

(23) Dessombz, A.; Chiche, D.; Davidson, P.; Panine, P.; Chanéac, C.; Jolivet, J. P. Design of Liquid-Crystalline Aqueous Suspensions of Rutile Nanorods: Evidence of Anisotropic Photocatalytic Properties. *J. Am. Chem. Soc.* **2007**, *129*, 5904−5909.

(24) Kato, T.; Gupta, M.; Yamaguchi, D.; Gan, K. P.; Nakayama, M. Supramolecular Association and Nanostructure Formation of Liquid Crystals and Polymers for New Functional Materials. *Bull. Chem. Soc. Jpn.* **2021**, *94*, 357−376.

(25) Arakaki, A.; Shimizu, K.; Oda, M.; Sakamoto, T.; Nishimura, T.; Kato, T. Biomineralization-Inspired Synthesis of Functional Organic/Inorganic Hybrid Materials: Organic Molecular Control of Self-Organization of Hybrids. *Org. Biomol. Chem.* **2015**, *13*, 974−989.

(26) Kato, T.; Sakamoto, T.; Nishimura, T. Macromolecular Templating for the Formation of Inorganic-Organic Hybrid Structures. *MRS Bull.* **2010**, *35*, 127−132.

(27) Suzuki, M.; Saruwatari, K.; Kogure, T.; Yamamoto, Y.; Nishimura, T.; Kato, T.; Nagasawa, H. An Acidic Matrix Protein, Pif, Is a Key Macromolecule for Nacre Formation. *Science* **2009**, *325*, 1388−1390.

(28) Sugawara, A.; Nishimura, T.; Yamamoto, Y.; Inoue, H.; Nagasawa, H.; Kato, T. Self-Organization of Oriented Calcium Carbonate/Polymer Composites: Effects of a Matrix Peptide Isolated from the Exoskeleton of a Crayfish. *Angew. Chem., Int. Ed.* **2006**, *45*, 2876−2879.

(29) Oaki, Y.; Kajiyama, S.; Nishimura, T.; Imai, H.; Kato, T. Nanosegregated Amorphous Composites of Calcium Carbonate and an Organic Polymer. *Adv. Mater.* **2008**, *20*, 3633−3637.

(30) Nakayama, M.; Kajiyama, S.; Kumamoto, A.; Ikuhara, Y.; Kato, T. Bioinspired Selective Synthesis of Liquid-Crystalline Nano-composites: Formation of Calcium Carbonate-Based Composite Nanodisks and Nanorods. *Nanoscale Adv.* **2020**, *2*, 2326−2332.

(31) Hoshino, T.; Nakayama, M.; Fujinami, S.; Nakatani, T.; Kohmura, Y.; Kato, T. Static Structure and Dynamical Behavior of Colloidal Liquid Crystals Consisting of Hydroxyapatite-Based Nano-rod Hybrids. *Soft Matter* **2019**, *15*, 3315−3322.

(32) Kajiyama, S.; Iwase, H.; Nakayama, M.; Ichikawa, R.; Yamaguchi, D.; Seto, H.; Kato, T. Shear-Induced Liquid-Crystalline Phase Transition Behaviour of Colloidal Solutions of Hydroxyapatite Nanorod Composites. *Nanoscale* **2020**, *12*, 11468−11479.

(33) Li, L. S.; Walda, J.; Manna, L.; Alivisatos, A. P. Semiconductor Nanorod Liquid Crystals. *Nano Lett.* **2002**, *2*, 557−560.

(34) Yang, Y.; Pei, H.; Chen, G.; Webb, K. T.; Martinez-Miranda, L. J.; Lloyd, I. K.; Lu, Z.; Liu, K.; Nie, Z. Phase Behaviors of Colloidal Analogs of Bent-Core Liquid Crystals. *Sci. Adv.* **2018**, *4*, No. eaas8829.

(35) Van Den Pol, E.; Petukhov, A. V.; Thies-Weesie, D. M. E.; Byelov, D. V.; Vroege, G. J. Experimental Realization of Biaxial Liquid Crystal Phases in Colloidal Dispersions of Boardlike Particles. *Phys. Rev. Lett.* **2009**, *103*, 258301.

(36) Kleshchanok, D.; Holmqvist, P.; Meijer, J. M.; Lekkerkerker, H. N. W. Lyotropic Smectic B Phase Formed in Suspensions of Charged Colloidal Platelets. *J. Am. Chem. Soc.* **2012**, *134*, 5985−5990.

(37) Miyamoto, N.; Nakato, T. Liquid Crystalline Inorganic Nanosheet Colloids Derived from Layered Materials. *Isr. J. Chem.* **2012**, *52*, 881−894.

(38) Onsager, L. The Effects of Shape on the Interaction of Colloidal Particles. *Ann. N.Y. Acad. Sci.* **1949**, *51*, 627−659.

(39) Jana, N. R.; Gearheart, L. A.; Obare, S. O.; Johnson, C. J.; Edler, K. J.; Mann, S.; Murphy, C. J. Liquid Crystalline Assemblies of Ordered Gold Nanorods. *J. Mater. Chem.* **2002**, *12*, 2909−2912.

(40) Woolston, P.; Van Duijneveldt, J. S. Isotropic-Nematic Phase Transition in Aqueous Sepiolite Suspensions. *J. Colloid Interface Sci.* **2015**, *437*, 65−70.

(41) Kim, J.; De La Cotte, A.; Deloncle, R.; Archambeau, S.; Biver, C.; Cano, J. P.; Lahlil, K.; Boilot, J. P.; Grelet, E.; Gacoin, T. LaPO$_4$ Mineral Liquid Crystalline Suspensions with Outstanding Colloidal Stability for Electro-Optical Applications. *Adv. Funct. Mater.* **2012**, *22*, 4949−4956.

(42) Zhang, S.; Majewski, P. W.; Keskar, G.; Pfefferle, L. D.; Osuji, C. O. Lyotropic Self-Assembly of High-Aspect-Ratio Semiconductor Nanowires of Single-Crystal ZnO. *Langmuir* **2011**, *27*, 11616−11621.

(43) Devol, R. T.; Sun, C. Y.; Marcus, M. A.; Coppersmith, S. N.; Myneni, S. C. B.; Gilbert, P. U. P. A. Nanoscale Transforming Mineral Phases in Fresh Nacre. *J. Am. Chem. Soc.* **2015**, *137*, 13325−13333.

(44) Mahamid, J.; Aichmayer, B.; Shimoni, E.; Ziblat, R.; Li, C.; Siegel, S.; Paris, O.; Fratzl, P.; Weiner, S.; Addadi, L. Mapping Amorphous Calcium Phosphate Transformation into Crystalline Mineral from the Cell to the Bone in Zebrafish Fin Rays. *Proc. Natl. Acad. Sci. U. S. A.* **2010**, *107*, 6316−6321.

(45) Weiner, S.; Addadi, L. Crystallization Pathways in Biomineraliza-tion. *Annu. Rev. Mater. Res.* **2011**, *41*, 21−40.

(46) Checa, A. G.; Cartwright, J. H. E.; Willinger, M.-G. The Key Role of the Surface Membrane in Why Gastropod Nacre Grows in Towers. *Proc. Natl. Acad. Sci. U. S. A.* **2009**, *106*, 38−43.

(47) Huang, W.; Shishehbor, M.; Guarín-Zapata, N.; Kirchhofer, N. D.; Li, J.; Cruz, L.; Wang, T.; Bhowmick, S.; Stauffer, D.; Manimunda, P.; Bozhilov, K. N.; Caldwell, R.; Zavattieri, P.; Kisailus, D. A Natural Impact-Resistant Bicontinuous Composite Nanoparticle Coating. *Nat. Mater.* **2020**, *19*, 1236−1243.

(48) Yao, H.-B.; Ge, J.; Mao, L.-B.; Yan, Y.-X.; Yu, S.-H. 25th Anniversary Article: Artificial Carbonate Nanocrystals and Layered Structural Nanocomposites Inspired by Nacre: Synthesis, Fabrication and Applications. *Adv. Mater.* **2014**, *26*, 163−188.

(49) De Yoreo, J. J.; Gilbert, P. U. P. A.; Sommerdijk, N. A. J. M.; Penn, R. L.; Whitelam, S.; Joester, D.; Zhang, H.; Rimer, J. D.; Navrotsky, A.; Banfield, J. F.; Wallace, A. F.; Michel, F. M.; Meldrum, F. C.; Cölfen, H.; Dove, P. M. Crystallization by Particle Attachment in Synthetic, Biogenic, and Geologic Environments. *Science* **2015**, *349*, aaa6760.

(50) Gal, A.; Kahil, K.; Vidavsky, N.; Devol, R. T.; Gilbert, P. U. P. A.; Fratzl, P.; Weiner, S.; Addadi, L. Particle Accretion Mechanism Underlies Biological Crystal Growth from an Amorphous Precursor Phase. *Adv. Funct. Mater.* **2014**, *24*, 5420−5426.

(51) Jehannin, M.; Rao, A.; Cölfen, H. New Horizons of Nonclassical Crystallization. *J. Am. Chem. Soc.* **2019**, *141*, 10120−10136.

(52) Cantaert, B.; Kuo, D.; Matsumura, S.; Nishimura, T.; Sakamoto, T.; Kato, T. Use of Amorphous Calcium Carbonate for the Design of New Materials. *ChemPlusChem* **2017**, *82*, 107−120.

(53) Kim, Y.-Y.; Douglas, E. P.; Gower, L. B. Patterning Inorganic (CaCO$_3$) Thin Films via a Polymer-Induced Liquid-Precursor Process. *Langmuir* **2007**, *23*, 4862−4870.

(54) Kim, Y.-Y.; Hetherington, N. B. J.; Noel, E. H.; Kröger, R.; Charnock, J. M.; Christenson, H. K.; Meldrum, F. C. Capillarity Creates

Single-Crystal Calcite Nanowires from Amorphous Calcium Carbonate. *Angew. Chem., Int. Ed.* **2011**, *123*, 12780−12785.

(55) Kato, T.; Suzuki, T.; Amamiya, T.; Irie, T.; Komiyama, M.; Yui, H. Effects of Macromolecules on the Crystallization of $CaCO_3$: the Formation of Organic/Inorganic Composites. *Supramol. Sci.* **1998**, *5*, 411−415.

(56) Wagner, J.; Märkert, C.; Fischer, B.; Müller, L. Direction Dependent Diffusion of Aligned Magnetic Rods by Means of X-Ray Photon Correlation Spectroscopy. *Phys. Rev. Lett.* **2013**, *110*, 048301.

(57) Sahu, A.; Choi, W. I.; Lee, J. H.; Tae, G. Graphene Oxide Mediated Delivery of Methylene Blue for Combined Photodynamic and Photothermal Therapy. *Biomaterials* **2013**, *34*, 6239−6248.

(58) Qin, M.; Hah, H. J.; Kim, G.; Nie, G.; Lee, Y. E. K.; Kopelman, R. Methylene Blue Covalently Loaded Polyacrylamide Nanoparticles for Enhanced Tumor-Targeted Photodynamic Therapy. *Photochem. Photobiol. Sci.* **2011**, *10*, 832−841.

(59) Venkataraman, S.; Hedrick, J. L.; Ong, Z. Y.; Yang, C.; Ee, P. L. R.; Hammond, P. T.; Yang, Y. Y. The Effects of Polymeric Nanostructure Shape on Drug Delivery. *Adv. Drug Delivery Rev.* **2011**, *63*, 1228−1246.

(60) Akiyama, J.; Hashimoto, M.; Takadama, H.; Nagata, F.; Yokogawa, Y.; Iwai, K.; Sassa, K.; Asai, S. Formation of C-Axis Aligned Polycrystal Hydroxyapatite Using a High Magnetic Field with Mechanical Sample Rotation. *Mater. Trans.* **2006**, *70*, 412−414.

(61) Liu, Y.; Li, Y.; Xue, G.; Cao, W.; Zhang, Z.; Wang, C.; Li, X. Shape Switching of $CaCO_3$-Templated Nanorods into Stiffness-Adjustable Nanocapsules to Promote Efficient Drug Delivery. *Acta Biomater.* **2021**, *128*, 474−485.

(62) Fan, W.; Qi, Y.; Wang, R.; Xu, C.; Zhao, N.; Xu, F. J. Calcium Carbonate-Methylene Blue Nanohybrids for Photodynamic Therapy and Ultrasound Imaging. *Sci. China Life Sci.* **2018**, *61*, 483−491.

(63) Wang, M.; He, L.; Zorba, S.; Yin, Y. Magnetically Actuated Liquid Crystals. *Nano Lett.* **2014**, *14*, 3966−3971.

(64) Song, X.; Tetik, H.; Jirakittsonthon, T.; Parandoush, P.; Yang, G.; Lee, D.; Ryu, S.; Lei, S.; Weiss, M. L.; Lin, D. Biomimetic 3D Printing of Hierarchical and Interconnected Porous Hydroxyapatite Structures with High Mechanical Strength for Bone Cell Culture. *Adv. Eng. Mater.* **2019**, *21*, 1800678.

(65) Minami, K.; Kasuya, Y.; Yamazaki, T.; Ji, Q.; Nakanishi, W.; Hill, J. P.; Sakai, H.; Ariga, K. Highly Ordered 1D Fullerene Crystals for Concurrent Control of Macroscopic Cellular Orientation and Differentiation toward Large-Scale Tissue Engineering. *Adv. Mater.* **2015**, *27*, 4020−4026.

(66) Nakayama, K. H.; Hong, G.; Lee, J. C.; Patel, J.; Edwards, B.; Zaitseva, T. S.; Paukshto, M. V.; Dai, H.; Cooke, J. P.; Woo, Y. J.; Huang, N. F. Aligned-Braided Nanofibrillar Scaffold with Endothelial Cells Enhances Arteriogenesis. *ACS Nano* **2015**, *9*, 6900−6908.

(67) Prévôt, M. E.; Ustunel, S.; Hegmann, E. Liquid Crystal Elastomers—A Path to Biocompatible and Biodegradable 3D-LCE Scaffolds for Tissue Regeneration. *Materials* **2018**, *11*, 377.